Cilt 9, Özel Sayı, Sayfa 141-147, 2020 Volume 9, Special Issue, Page 141-147, 2020

Araştırma Makalesi https://doi.org/10.46810/tdfd.744947 Research Article

Türk Doğa ve Fen Dergisi
Turkish Journal of Nature and Science
www.dergipark.gov.tr/tdfd

Physical characteristics of n-Si/GaN thin films: effect of different N rates

Asim MANTARCI[1*]

[1] Muş Alparslan Üniversitesi, Varto Meslek Yüksekokulu, Tıbbi Hizmetler ve Teknikler Bölümü, Muş, Türkiye
Asim MANTARCI ORCID No: 0000-0001-8369-3559

**Sorumlu yazar: a.mantarci@alparslan.edu.tr*

(Alınış: 29.05.2020, Kabul: 13.09.2020, Online Yayınlanma: 23.10.2020)

Keywords
RF sputter technique, GaN, N rate, III-nitrides

Abstract: The GaN thin film was fabricated on n-type Si by a Radio Frequency magnetron sputtering method with applied various nitrogen (N) rates. The XRD confirmed the produced film had in a polycrystalline structure (orientations (110) and (100)). It was seen that different N rates varied structural parameters of fabricated material. The optical analysis showed that various N rates changed thin film optical-band gap energy by reason of reduced N vacancy. The AFM pictures demonstrated almost homogeneous with periodic grain arrangements, Nano-structured surface of GaN thin film. From SEM pictures, we detected agglomerations on the surface of the GaN thin film. Possible causes of them were deeply discussed. Raman results proved the corresponding characteristic $E_2(\text{high})$ peak of the hexagonal GaN and exhibited that all thin films had tensile stress. Reasons of this stress were discussed. Optical, morphological, structural parameters of GaN thin film can be improved with controlling N rates. Produced thin films can be basic material in device applications such as solar cells, Light Emitting Diode (LED).

n-Si / GaN ince filmlerin fiziksel özellikleri: farklı N oranı etkisi

Keywords
RF saçtırma tekniği, GaN, N oranı, III-nitrür

Öz: GaN ince filmi, Radyo Frekansı magnetron saçtırma yöntemi ile n-tipi Si üzerinde farklı N oranları uygulanarak üretildi. XRD analizleri üretilen filmin polikristal yapıda olduğunu (oryantasyon (110) ve (100)) teyit etmiştir. Farklı N oranlarında malzemenin yapısal parametrelerinin değiştiği görülmektedir. Optik analiz, çeşitli N oranlarının Azot boşluğunun azalması nedeniyle ince film optik bant boşluk enerjisini değiştirdiğini göstermektedir. AFM resimleri, GaN ince filminin Nano yapılı bir yüzeye sahip olduğunu ve periyodik tanecik yapısı gösterdiğini neredeyse homojen olan yapıyı göstermiştir. SEM resimlerinden GaN ince filminin yüzeyinde topaklar tespit ettik. Bunların olası nedenleri detaylı tartışıldı. Raman sonuçları, altıgen GaN'nin karşılık gelen karakteristik E_2 (yüksek) optic fonon titreşimini kanıtlamıştır ve tüm ince filmlerin sıkıştırma gerginliğine sahip olduğunu göstermiştir. Filmde oluşan bu stresin nedenleri tartışıldı. GaN ince filmin optik, morfolojik, yapısal parametreleri N oranlarının kontrol edilmesiyle iyileştirilebildiği bulunmuştur. Üretilen ince filmler, güneş pilleri, Işık Yayan Diyot (LED) gibi cihaz uygulamalarında temel malzeme olabilmektedir.

1. INTRODUCTION

Semiconductors of III-nitrides have been an important field of study to develop devices in optoelectronic applications [1]. Lately, several researchers studied them to apply high technology [2]. Gallium Nitride (GaN) has been material from group of III-nitrides and has noteworthy physical parameters (thermal stability, direct-wide bandgap, high-melting-point [3] high electron mobility [4], high breakdown voltage [5], mechanical hardness. This material has become an important material in the industry due to the above-mentioned properties. It can be listed as; solar-cell [6-7], pH sensor [8], LED device [9], beta voltaic device [10].

In this article, N rates effect on physical parameters of $n-Si/GaN$ thin film using Radio Frequency magnetron sputtering were deeply studied. We have two main contributions for this work. From our detailed literature review, impacts of various N rates on physical parameters $n-Si/GaN$ thin film using Radio Frequency magnetron sputter method has not been investigated. In addition to this; nitrogen deficiency has been one of the

problems encountered in growing GaN thin films. This causes in the GaN material being of lower quality and this has been other reason to research the N rates effect on growth and characterization of GaN thin film.

2. MATERIAL AND METHOD

The working mechanism of the RF sputtering technique was explained in detail in the reference [11]. We used RF magnetron sputter machine (PVD-Midas 3M) to produce films at DAYTAM (East Anatolian High Technology Application and Research Center). To remove contaminations, a turbo molecular pump and a mechanical pump was used. GaN target with purity 99.99% (4N) and with $2^{\text{ıı}}$ dia $\times 0.125^{\text{ıı}}$ thick (lot no: 22709-16-02) was provided from ACI Alloys company. We purchased $n-Si(100)$ (as substrate) (Sigma Aldrich Chemistry Company). The following processes were carried out before the thin-film growth step. Substrates used were carefully cut the diamond cutter. Before growing thin films, RCA-1 (Radio Corporation America-1) and RCA-2 (Radio Corporation America-2) cleaning procedures were applied. Also, 75 Watt Radio Frequency power was applied to our system. Argon gas was applied at a rate of 75 sccm as growth gas. Nitrogen gas was supplied to the system at $0, 1, 2, 3, 4$ sccm to study the effect of N rates. Applied growth conditions for films were given (in Table 1). International Organization for Standardization class (ISO-3) cleaning standards for all growth, cleaning, and preparation processes were followed. Also, GaN thin film's thicknesses were measured using surface profile metrology P7 (KLA-Tencor). Thin films' thicknesses were measured with a sensor (inside of the system). By comparing these values, calibration was done by a profile meter. Micro-Raman (alpha300 R) spectrometer was used to analyze optical parameters. Using UV/Vis/NIR Spectrophotometer (LAMBDA 1050), an optical bandgap analysis of thin films was performed. Field-Emission Scanning Electron Microscopy (FE-SEM) (Zeiss Sigma300model) was studied to analyze the surface of films. Morphological analysis of GaN thin films was studied using AFM-500II. X-ray Diffraction System (PANalytical Empyrean) was implemented ($CuK_{\alpha} = 1.5406\ A^{\circ}$) to study of the film's structure. DAYTAM facilities were used for whole growth and characterization processes.

Table 1. Applied growth condition for films

N Rates $(sccm)$	RF Power $(Watt)$	Base Pressure (kPa)	Working Pressure (kPa)	Film' Thickness (nm)	Growth Rate $(A^{\circ}/_{S})$	Substrate Temperature (C°)
0	75	0.14×10^{-6}	0.87×10^{-3}	110	0.3	300
1	75	0.26×10^{-6}	0.86×10^{-3}	110	0.3	300
2	75	1.09×10^{-7}	0.89×10^{-3}	110	0.3	300
3	75	1.15×10^{-7}	0.83×10^{-3}	110	0.3	300
4	75	0.27×10^{-6}	0.87×10^{-3}	110	0.3	300

3. RESULTS AND DISCUSSIONS

3.1. XRD Phase Study

Fig. 1 gives XRD spectra of $GaN/n-Si$ thin films. The peak of 32.40° was detected for all N rates, which was corresponded to hexagonal GaN (100) plane (ICSD-PDF: 01-076-0703 [12]). The peak of 61.19° was observed for all nitrogen values also, which was corresponded to hexagonal GaN (110) plane (ICSD-PDF: 01-079-2499 [13]).

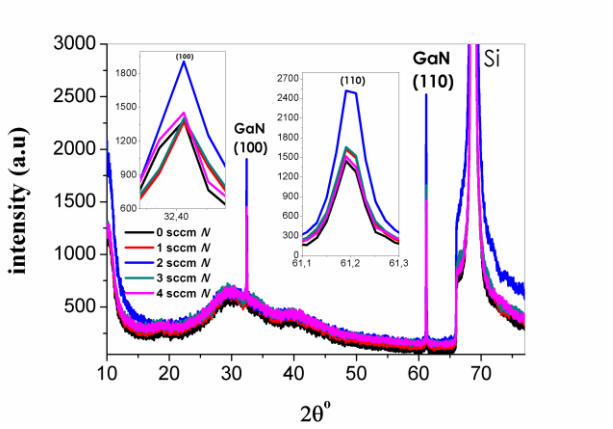

Figure 1 XRD spectra of GaN/n-Si thin films

X-ray diffraction measurements confirmed that GaN thin films have a hexagonal polycrystalline structure ((100) and (110) planes). 59.70° peak changed to 61.19° for (110) planes of hexagonal GaN. These shifts can be originated from impurities in the thin films. As expected, we observed a peak at ~69° belonging to Si, in agreement with the literature [14]. Thin-film grain size values can be found by Scherrer formula;

$$D = {M\lambda}/{\beta Cos\theta} \qquad (1)$$

λ shows X-ray wavelength, M = 0.9 shows the constant, β shows FWHM intensity, θ shows Bragg's diffraction angle. Table 2 gives detailed structural parameters of thin films at different N rates.

Table 2 Detailed structural parameters of films

N Rates (*sccm*)	(*hkl*)	FWHM (°)	2θ (Observed) (°)	2θ (*) (°)	d-values (Å)	d-values (*) (Å)	Lattice parameters (*) (Å)	Lattice parameters (Å)	Grain size (D) (*nm*)
0	(100)	0.1580	32.40	32.38	2.7599	2.7626	$a = 3.1900$ $c = 5.1890$	$a = 3.1868$ $c = 5.2041$	54.67
	(110)	0.1571	61.19	59.70	1.5129	1.5475	$a = 3.0950$ $c = 5.0000$	$a = 3.0258$ $c = 4.9411$	61.34
1	(100)	0.2611	32.40	32.38	2.7599	2.7626	$a = 3.1900$ $c = 5.1890$	$a = 3.1868$ $c = 5.2041$	33.08
	(110)	0.2618	61.19	59.70	1.5129	1.5475	$a = 3.0950$ $c = 5.0000$	$a = 3.0258$ $c = 4.9411$	36.81
2	(100)	0.1570	32.40	32.38	2.7599	2.7626	$a = 3.1900$ $c = 5.1890$	$a = 3.1868$ $c = 5.2041$	55.01
	(110)	0.1563	61.19	59.70	1.5129	1.5475	$a = 3.0950$ $c = 5.0000$	$a = 3.0258$ $c = 4.9411$	61.65
3	(100)	0.1630	32.40	32.38	2.7599	2.7626	$a = 3.1900$ $c = 5.1890$	$a = 3.1868$ $c = 5.2041$	52.99
	(110)	0.1625	61.19	59.70	1.5129	1.5475	$a = 3.0950$ $c = 5.0000$	$a = 3.0258$ $c = 4.9411$	59.30
4	(100)	0.1425	32.40	32.38	2.7599	2.7626	$a = 3.1900$ $c = 5.1890$	$a = 3.1868$ $c = 5.2041$	60.61
	(110)	0.1427	61.19	59.70	1.5129	1.5475	$a = 3.0950$ $c = 5.0000$	$a = 3.0258$ $c = 4.9411$	67.53

*(PDF#01-076-0703, 01-079-2499)

N rate increasing from 0 sccm to 1 sccm led to that FWHM was increased and the grain size of the material was decreased. On the other hand, N rate increasing from 1 sccm to 2 sccm led to that FWHM was decreased and the grain size of our material was increased. N rate increasing from 2 sccm to 3 sccm led to that FWHM was increased and grain size of the material was decreased. But N rate increasing from 3 sccm to 4 sccm led to that FWHM was decreased and grain size of the material was increased. The result of a change of grain sizes can be explained; increase in grain size at increased N rate (from 1 sccm to 2 sccm and from 3 sccm to 4 sccm) can be attributed to energetic ion bombardment enhancement due to excess N as dominant mechanism. This increases mobility of ad-atoms. This leads to an increase in grain size. But increase in grain size at increased N rate (from 0 sccm to 1 sccm and from 2 sccm to 3 sccm) can be related to energetic ion bombardment decrement due to excess N as dominant mechanism. This decreases mobility of ad-atoms. This results in a decrement in thin film's grain size. Overall, it has achieved two main results. One has been that the structural properties (FWHM, grain size) of our material showed non-linear changes with N rates, as shown in Figure 2 clearly.

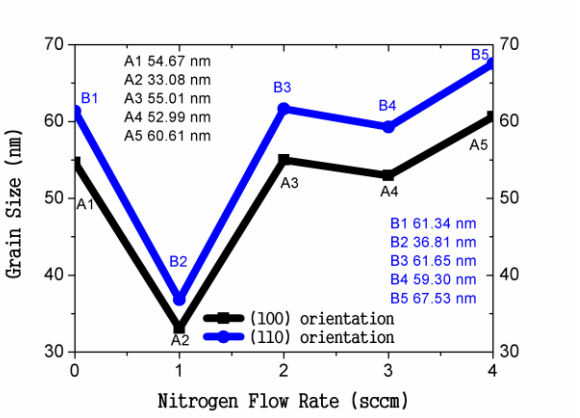

Figure 2. Grain sizes of (100) and (110) plane for various N rates.

Other has been that it was found that the highest grain size value in the structure of GaN/n − Si thin film for both planes was achieved under 4 sccm N rate and the lowest grain size value in structure of GaN/n − Si thin film for both planes was achieved under 1 sccm N rate.

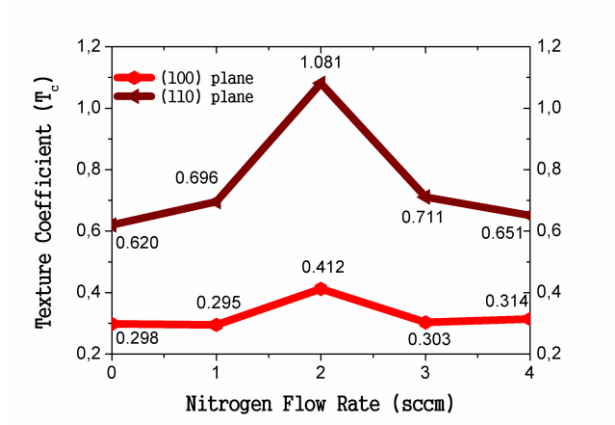

Figure 3 Texture coefficients (T_c) versus various N rates.

The texture coefficient (T_c) of the material was found by Harris-texture relation;

$$T_{c_{(hkl)}} = \frac{{}^{I_{(hkl)}}/_{I_{0_{(hkl)}}}}{({}^{1}/_{N})[\sum_{N}({}^{I_{(hkl)}}/_{I_{0_{(hkl)}}})]} \quad (2)$$

$T_{c_{(hkl)}}$ shows the texture coefficient ((hkl) plane), $I_{(hkl)}$ shows XRD measurement intensity, $I_{0_{(hkl)}}$ shows relative intensity for (hkl) plane from corresponding PDF code, N shows the number of reflections. Table 3 gives the texture coefficient and the corresponding plane.

Table 3. Texture coefficient for each plane

N Rates ($sccm$)	(hkl)	Measured Intensity ($I_{(hkl)}$)	Relative Intensity ($I_{0_{(hkl)}}$)	Texture Coefficient (T_c)
0	(100)	1382	4630	0.298
	(110)	1445	2330	0.620
1	(100)	1370	4630	0.295
	(110)	1624	2330	0.696
2	(100)	1908	4630	0.412
	(110)	2520	2330	1.081
3	(100)	1404	4630	0.303
	(110)	1658	2330	0.711
4	(100)	1454	4630	0.314
	(110)	1517	2330	0.651

The N rate increasing from 0 sccm to 1 sccm lead to the texture coefficient value decreased for (100) plane. The N rate increasing from 1 sccm to 2 sccm results in that texture coefficient value increased for (100) plane. The N rate increasing from 2 sccm to 3 sccm lead to the texture coefficient value decreased for (100) plane. The N rate increasing from 3 sccm to 4 sccm results in that texture coefficient value increased for (100) plane. As for (110) plane, the N rate increasing from 0 sccm to 1 sccm lead to texture coefficient value increased. The N rate increasing from 1 sccm to 2 sccm result in that texture coefficient value increased for (110) plane. The N rate increasing from 2 sccm to 3 sccm lead to texture coefficient value decreased. Also, the N rate increasing from 3 sccm to 4 sccm lead to texture coefficient value decreased (Figure 3). As a result, at 2 sccm N rate, the highest texture coefficient for both planes was obtained. A large number of crystallites are oriented by their (hkl) planes in the direction of the specific crystalline plane if the texture coefficient is bigger than 1. If the texture coefficient is close to 1, it tells more random orientation. If the texture coefficient is between $0-1$, it shows grain orientation fault toward the considered plane. Lattice parameters c and a can be calculated with formula 3 (Bragg formula) and 4 ;

$$d_{hkl} = {}^{\lambda}/_{(2sin\Theta_{hkl})} \quad (3)$$

$$\frac{1}{d_{hkl}} = \sqrt{\frac{4}{3}\left(\frac{h^2+h.k+k^2}{a^2}\right)+\frac{l^2}{c^2}} \quad (4)$$

a and c are the lattice parameters for hexagonal material, d is the space of lattice, hkl is the miller indices, Θ_{hkl} is the reflection angle from hkl miller indices, λ is the wavelength of X-ray source. Lattice constants of material are shown in Tab.2. From XRD results, it was concluded that the structural properties (FWHM, grain size, texture coefficient) of material showed non-linear behavior with N rate, as given Figure 2 and Figure 3. Also, at 2 sccm N rate, the highest texture coefficient for both planes was obtained.

3.2. Morphological Analysis by AFM

Figure 4 presents Atomic Force Microscopy images of material. The maximum depth (R_v) of material was 2.27 nm (the lowest value, 3 sccm flow rate). The maximum depth (R_v) of material was 8.19 nm (the highest value, the flow rate of 0 sccm), as showing in Figure 5.

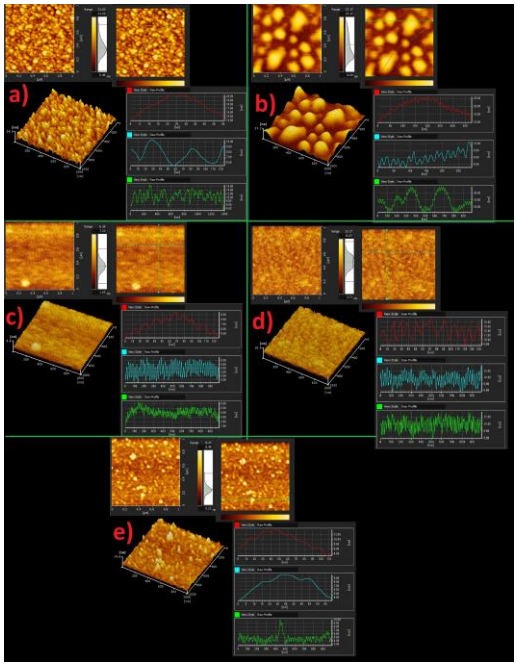

Figure 4. Atomic Force Microscopy images under **a)** 0 **b)** 1 **c)** 2 **d)** 3 **e)** 4 sccm N flow rates.

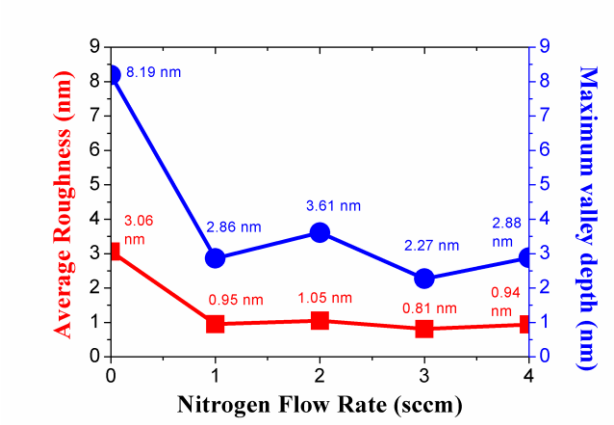

Figure 5. N rates & maximum valley depth and roughness

The highest average absolute slope (Δa) was 12.74° related to 0 sccm N rate. The lowest average absolute slope was 6.08° related to 2 sccm N rate. Maximum height of GaN thin film on n − Si substrate was 14.68 nm (the highest value) corresponding to 0 sccm N rate. Maximum height of material was 2.65 nm (the lowest value) corresponding to 1 sccm N rate. Table 4 gives surface properties of our material.

Table 4. Surface properties of materials

N Rates $(sccm)$	Average Roughness $(R_a)(nm)$	Maximum peak height $(R_p)(nm)$	Average-Absolute slope $(\Delta a)(°)$	Maximum-Valley depth $(R_v)(nm)$
0	3.06	14.88	12.74	8.19
1	0.95	2.65	8.44	2.86
2	1.05	3.73	6.08	3.61
3	0.81	3.08	7.73	2.27
4	0.94	2.95	8.46	2.88

N rate increasing from 0 sccm to 1 sccm led to a smoother surface (2.11 nm). However; the N rate increasing from 1 sccm to 2 sccm led to a rougher surface (0.10 nm). The N rate increasing from 2 sccm to 3 sccm led to a smoother surface (0.24 nm). The N rate increasing from 3 sccm to 4 sccm led to a rougher surface (0.13 nm . Our film's roughness ranged from 0.81 nm to 3.06 nm. 3.06 nm was the highest average roughness related to 0 sccm N rate, 0.81 nm was the lowest average roughness related to 3 sccm N rate. Morphologically desired thin film was obtained under the N rate of 3 sccm with the lowest roughness. The N rate increasing from 0 sccm to 1 sccm led to a decrease in roughness. Surface morphology of the material was improved. However; the Nrate increasing from 1 sccm to 2 sccm led to a slight increase in roughness. Surface morphology of the material was deteriorated. N rate increasing from 2 sccm to 3 sccm led to a slight decrease in roughness. Surface morphology of our material was improved. But; N rate increasing from 3 sccm to 4 sccm led to a slight increase in roughness. Surface morphology of material was deteriorated. The AFM pictures demonstrated almost homogeneous with periodic grain arrangements, Nano-structured GaN film surface. It was concluded surface parameters of material exhibit non-linear behavior with N rate.

3.3. SEM Analysis

In order to investigate surface properties of the material, SEM measurement (secondary electron mode) was taken. 40.00 KX Magnification was used in the measurements. Figure 6 gives the material's Scanning Electron Microscopy images with a magnification of 40.00 KX for varied N rates.

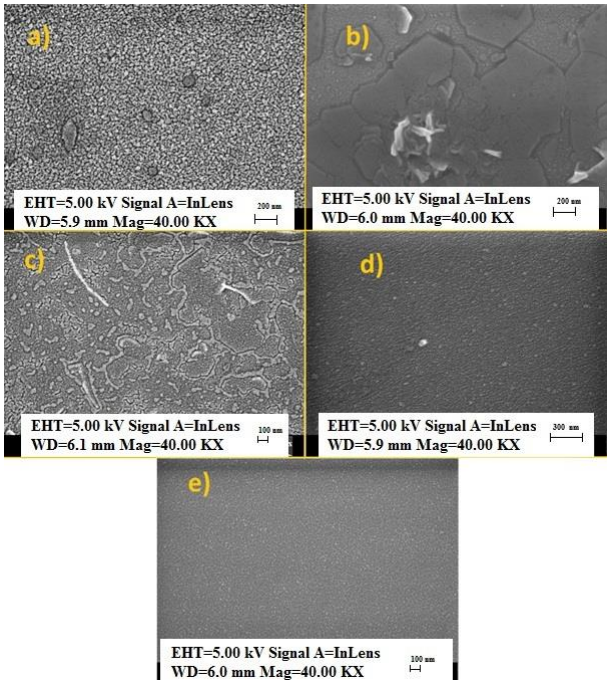

Figure 6 The material's Scanning Electron Microscopy images (40.00 KX magnification) a) 0 b) 1 c) 2 d) 3 e) 4 sccm N rates

The surface of the material at 0 $sccm$ N rate exhibited some agglomerations due to van der Waals interaction between particles [15]. N rate increasing from 0 sccm to 1 sccm caused to that the material surface is distorted. When N rate was increased to 1 $sccm$ and 2 $sccm$, it was seen that the material surface had some agglomerations. N rate increasing from 2 sccm to 3 sccm led to improvement of GaN thin film surface. The surface of the material exhibits an almost-homogenous structure. The N rate increasing from 3 sccm to 4 sccm caused to more improvement of GaN thin film surface. Also the grains on the material surface appear clearer. From evaluation of SEM measurements, it can be said that the best morphology in terms of surface homogeneity and clarity was obtained from N rate of 4 $sccm$. Also, changing the grain size with various N rate was supported by SEM images. Surface parameters of the material exhibited non-linear changes with different N rates.

3.4. Optical Properties Study

3.4.1. Optical bandgap energy

The material's optical bandgap energies were estimated using Tauc relation;

$$(\alpha h\nu)^r = Z(h\nu - E_g) \quad (6)$$

Where Z shows the constant value, r shows bandgap type, and E_g shows optical bandgap energy of the material, hν shows photon energy. E_g gives direct-allowed bandgap energy of the material when $r = 1/2$. Fig. 7 presents $(\alpha h\nu)^2$ & E of the material for different N rates.

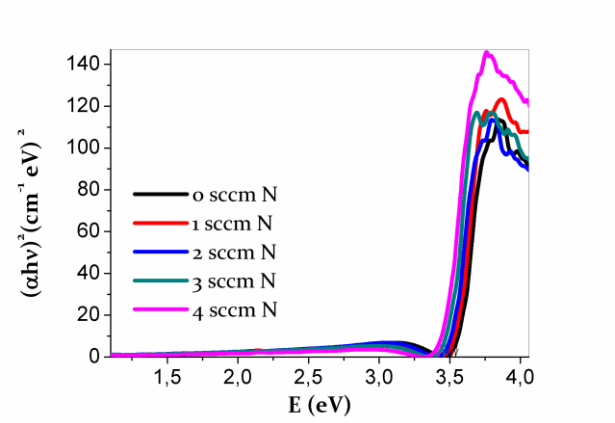

Figure 7 $(\alpha h\nu)^2$ & E of the material for different N rates

For $(\alpha h\nu)^2 = 0$, linear lines were plotted to achieve optical bandgap of the material. E_g values of the material were obtained to be 3.54, 3.51, 3.48, 3.45, 3.41 eV for $0, 1, 2\ 3, 4$ sccm, respectively, giving in Table 5.

Table 5. E(g) values of materials

N Rates ($sccm$)	**Optical bandgap energy** (eV)
0	3.54
1	3.51
2	3.48
3	3.45
4	3.41

Increased N rate leads to a decrease in optical bandgap energy of the material. Reason for this can be explained as follows. N vacancy defects in GaN thin film leads to an increase in optical band gap of GaN thin film in literature study [16]. A change in thin-film optical bandgap energy could be due to a decrease in the N vacancy defect. Our optical bandgap energy values are found to be close to those in past studies [17].

3.4.2. Residual stress and optical-phonon modes

Group theory says that hexagonal GaN (belonged to C_{6v}^4 space group) possess Raman active modes of six ($1E_1\,(TO) + 1E_1\,(LO) + 2E_2 + 1A_1\,(TO) + 1A_1\,(LO)$). Raman spectrum of $GaN/n-Si$ thin films under various N rates is displayed in Figure 8.

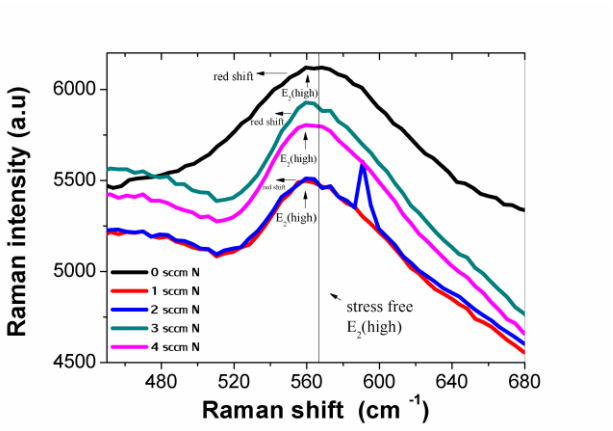

Figure 8 Raman results for different N rates

We detected peaks at 559.4908, 559.9355, 559.6885, 559.4908, 559.5896 cm^{-1} for 0, 1, 2, 3, 4 sccm N rate. The peaks observed correspond to the E_2 (high) [18] optical phonon mode. The highest Raman intensity was found at 0 sccm N rate. However, the lowest Raman intensity was found at 1 sccm N rate. We concluded that effects of plasmon-phonon coupling and the effects of surface states [19] can be a reason for higher Raman intensity. Mechanical parameters of thin-film have occupied an important place in device production. Therefore, controlling them has become very crucial to be able to fabricate high-quality device. GaN thin film stress free Raman shift of $E_2(high)$ was determined to be 567.2 cm^{-1} at previous investigation [20]. Thin-film feels compressive stress if the Raman shift is higher than stress free Raman shift of $E_2(high)$. It is called blue shift. But, if Raman shift is lower than stress free Raman shift of $E_2(high)$, thin-film feels tensile stress. It is called a red shift. Raman shift of $E_2(high)$ was in the red region at all nitrogen gas flow rates, proving all films had a tensile stress. The reasons for this stress are given as follows. Lattice constants of $n-Si$ and GaN are different ($a_{n-Si} = 5.4037$ Å and for lattice constant of GaN, see Tab.2). Another factor is the thermal expansion coefficient difference ($\alpha_{GaN} = 5.6 \times 10^{-6}K^{-1}$, $\alpha_{n-Si} = \sim 2.6 \times 10^{-6}K^{-1}$). We grow thin film at 300 ℃ substrate temperature. During the growth process, films are expanding at different ratios due to the thermal expansion coefficient difference. After the cooled down process, films occurred stress in it. In conclusion, residual stress in GaN thin film has been significant in device fabrication. The separation layer in a device is formed due to compressive stress in films. This leads to a short-circuited in the material. A cracking in films is formed due to tensile stress. This leads to a limitation of the sheet usable thickness. In brief, the change in N rate has an influence on optical phonon modes.

4. CONCLUSION

Polycrystalline-hexagonal GaN (orientations (110) and (100)) thin film was successfully fabricated. The highest and the lowest grain size value of $GaN/n-Si$ thin film for both planes were obtained 4 sccm N rate and 1 sccm N rate, the optimal value to obtain highest grain size in our thin film was 4 sccm N rate among the applied values. At 2 sccm N rate, the highest texture

coefficient for both planes was obtained. It was concluded that surface parameters of the material exhibited non-linear behavior with N rate. Increased N rate leads to a decrease in thin film optical bandgap energy. It could be due to a decrease in N vacancy defect. The surface of the material at 0 sccm N rate exhibited some agglomerations due to van der Waals interaction between particles. E_2(high) optical phonon mode was detected from Raman measurements. Also, the Raman peak shifted to the red region, confirming all films felt tensile stress due to thermal coefficient difference and the lattice parameter difference. These results may contribute to high-quality device production.

REFERENCES

[1] Hu X-l, Wen R-l, Qi Z-y, Wang H. III-nitride ultraviolet, blue and green LEDs with SiO2 photonic crystals fabricated by UV-nanoimprint lithography. Materials Science in Semiconductor Processing. 2018;79:61-5. doi: 10.1016/j.mssp.2018.01.024.

[2] Mohanty G, Sahoo BK. Effect of III-V nitrides on performance of graphene based SPR biosensor for detection of hemoglobin in human blood sample: A comparative analysis. Current Applied Physics. 2016;16(12):1607-13. doi: 10.1016/j.cap.2016.09.006.

[3] Moon WH, Kim HJ, Choi CH. Molecular dynamics simulation of melting behavior of GaN nanowires. Scripta Materialia. 2007;56(5):345-8. doi: 10.1016/j.scriptamat.2006.11.013.

[4] He XG, Zhao DG, Jiang DS, Zhu JJ, Chen P, Liu ZS, et al. GaN high electron mobility transistors with AlInN back barriers. Journal of Alloys and Compounds. 2016;662:16-9. doi: 10.1016/j.jallcom.2015.12.031.

[5] Saito W, Suwa T, Uchihara T, Naka T, Kobayashi T. Breakdown behaviour of high-voltage GaN-HEMTs. Microelectronics Reliability. 2015;55(9):1682-6. doi: 10.1016/j.microrel.2015.06.126.

[6] Miyoshi M, Tsutsumi T, Kabata T, Mori T, Egawa T. Effect of well layer thickness on quantum and energy conversion efficiencies for InGaN/GaN multiple quantum well solar cells. Solid-State Electronics. 2017;129:29-34. doi: 10.1016/j.sse.2016.12.009.

[7] Sheu J-K, Chen P-C, Shin C-L, Lee M-L, Liao P-H, Lai W-C. Manganese-doped AlGaN/GaN heterojunction solar cells with intermediate band absorption. Solar Energy Materials and Solar Cells. 2016;157:727-32. doi: 10.1016/j.solmat.2016.07.047.

[8] Dong Y, Son D-h, Dai Q, Lee J-H, Won C-H, Kim J-G, et al. AlGaN/GaN heterostructure pH sensor with multi-sensing segments. Sensors and Actuators B: Chemical. 2018;260:134-9. doi: 10.1016/j.snb.2017.12.188.

[9] Liu Z, Chong WC, Wong KM, Lau KM. GaN-based LED micro-displays for wearable applications. Microelectronic Engineering. 2015;148:98-103. doi: 10.1016/j.mee.2015.09.007.

[10] Lin J-H, Huang S-J, Su Y-K, Huang K-W. The improvement of GaN-based LED grown on concave nano-pattern sapphire substrate with SiO2 blocking layer. Applied Surface Science. 2015;354:168-72. doi: 10.1016/j.apsusc.2015.02.151.

[11] Abud SH, Selman AM, Hassan Z. Investigation of structural and optical properties of GaN on flat and porous silicon. Superlattices and Microstructures. 2016;97:586-90. doi: 10.1016/j.spmi.2016.07.017.

[12] Schulz H, Thiemann KH. Crystal structure refinement of AlN and GaN. Solid State Communications. 1977;23(11):815-9. doi: 10.1016/0038-1098(77)90959-0.

[13] Yeh C-Y, Lu ZW, Froyen S, Zunger A. Zinc-blende\char21{}wurtzite polytypism in semiconductors. Physical Review B. 1992;46(16):10086-97. doi: 10.1103/PhysRevB.46.10086.

[14] Miyoshi M, Tsutsumi T, Kabata T, Mori T, Egawa T. Effect of well layer thickness on quantum and energy conversion efficiencies for InGaN/GaN multiple quantum well solar cells. Solid-State Electronics. 2017;129:29-34. doi: 10.1016/j.sse.2016.12.009.

[15] Kudrawiec R, Nyk M, Syperek M, Podhorodecki A, Misiewicz J, Strek W. Photoluminescence from GaN nanopowder: The size effect associated with the surface-to-volume ratio. Applied Physics Letters. 2006;88(18):181916. doi: 10.1063/1.2199489.

[16] Li J, Liu H, Wu L. The optical properties of GaN (001)surface modified by intrinsic defects from density functional theory calculation. Optik - International Journal for Light and Electron Optics. 2018;154:378-82. doi: 10.1016/j.ijleo.2017.10.040.

[17] Said A, Debbichi M, Said M. Theoretical study of electronic and optical properties of BN, GaN and B x Ga 1− x N in zinc blende and wurtzite structures. Optik-International Journal for Light and Electron Optics. 2016;127(20):9212-21. doi: 10.1016/j.ijleo.2016.06.103.

[18] Harima H. Properties of GaN and related compounds studied by means of Raman scattering. Journal of Physics: Condensed Matter. 2002;14(38):R967. doi: 10.1088/0953-8984/14/38/201.

[19] Sekine T, Komatsu Y, Iwaya R, Kuroe H, Kikuchi A, Kishino K. Surface Phonons Studied by Raman Scattering in GaN Nanostructures. Journal of the Physical Society of Japan. 2017;86(7):074602. doi: 10.7566/JPSJ.86.074602.

[20] Nootz G, Schulte A, Chernyak L, Osinsky A, Jasinski J, Benamara M, et al. Correlations between spatially resolved Raman shifts and dislocation density in GaN films. Applied Physics Letters. 2002;80(8):1355-7. doi: 10.1063/1.1449523.